Rare Met. (2022) 41(2):663–672
https://doi.org/10.1007/s12598-021-01786-1

RARE METALS

ORIGINAL ARTICLE

Polydopamine modified CuS@HKUST for rapid sterilization through enhanced photothermal property and photocatalytic ability

Dong-Lin Han*, Peng-Li Yu, Xiang-Mei Liu*, Ying-De Xu, Shui-Lin Wu*

Received: 9 March 2021 / Revised: 7 April 2021 / Accepted: 19 April 2021 / Published online: 30 June 2021

Abstract Because of the impressive evolution of the drug-resistant bacteria, the development of efficient, antibiotic-free agent is in great urgency. Herein, an efficient antibacterial agent, CuS@HKUST-polydopamine (PDA), was exquisitely designed, where the Cu-based metal-organic framework (MOF)—HKUST nanoparticles served as the porous frame, and the CuS was synthesized within the structure of the MOF through the process of in situ sulfuration, followed with polydopamine (PDA) covering the nanoparticles. The structure of the HKUST preventing the aggregation of the CuS nanoparticles, which improved their photothermal and photocatalytic properties. After covering with PDA, the nanoparticles' abilities to produce heat and free radicals were further enhanced. This was because that the PDA itself could transform light into heat, which not only benefited the photothermal property, but also improved the photocatalytic property of the nanoparticles by accelerating the charge mobility. Moreover, the PDA could also transfer the photo-induced electrons fast and thus prevented the recombination of the photo-generated electron–hole pairs, which resulted in the enhanced ability to produce free radicals. As a result, under light irradiation, the antibacterial efficiency of the CuS@HKUST-PDA against Staphylococcus aureus (*S. aureus*) and Escherichia coli (*E. coli*) could reach 99.77% and 99.57%. Hence, the synthesized CuS@HKUST-PDA can be promising for anti-infection and sterilization application without using antibiotics.

Keywords Antibacterial; CuS; Polydopamine (PDA); Photothermal; Photocatalytic; Metal-organic framework (MOF)

1 Introduction

Pathogenic bacteria exist everywhere in people's daily life, and always threaten people's health, even lives by polluting the drinking water, contaminating the wound healing environment, etc. [1, 2]. Along with the discovery of antibiotics, people found our way to defeat against these bacteria. However, in recent decades, because of the wide and immoderate use of antibiotics, the drug-resistance bacteria gradually appeared in the daily life [3, 4]. Some of these drug-resistance bacteria even could ignore the attack from the latest generations of penicillin and cephalosporins and become deadly to people again [5]. In order to slow the evolution of the drug-resistance bacteria, the development of some new, effective and non-antibiotic bacteria-killing methods is in great demand.

Under light irradiation, some materials could produce lots of heat and free radicals, and these photothermal and

Supplementary Information The online version contains supplementary material available at https://doi.org/10.1007/s12598-021-01786-1.

D.-L. Han*
College of Materials Science and Engineering, Jilin Institute of Chemical Technology, Jilin 132022, China
e-mail: han_donglin@tju.edu.cn

P.-L. Yu, Y.-D. Xu, S.-L. Wu*
School of Materials Science and Engineering, the Key Laboratory of Advanced Ceramics and Machining Technology by the Ministry of Education of China, Tianjin University, Tianjin 300072, China
e-mail: shuilinwu@tju.edu.cn

X.-M. Liu*
Ministry-of-Education Key Laboratory for the Green Preparation and Application of Functional Materials, Hubei Key Laboratory of Polymer Materials, School of Materials Science and Engineering, Hubei University, Wuhan 430062, China
e-mail: liuxiangmei1978@163.com

photocatalytic materials could help with energy storage, environment cleaning, treatment of disease, etc. [6, 7]. In the field of bacterial killing, the photothermal and photodynamic treatments have also been attracting more and more attentions [8–11], because they are environmentally friendly, nondestructive. And these MOF materials are also suitable for a variety of situations, such as environment cleaning [11], wound healing [12], and gas separation [13]. CuS, as a kind of semiconductor photosensitizer, not only could absorb light and produce heat through the d-d* transition and plasmon resonance, but also could produce free radicals under light irradiation, which shows great potential to act as a photosensitizer to kill bacteria. Furthermore, the CuS nanoparticles are also cheap, easy to be synthesized, and chemically stable, so they have attracted considerable attentions [14]. However, the pure CuS nanoparticles are easy to gather together, which decreases their photothermal and photocatalytic properties and finally leads to the decreased antibacterial property [1, 15]. So, it is necessary to design effective carriers to prevent the aggregation of the CuS nanoparticles, thus guaranteeing their high ability to produce heat and free radicals. HKUST, a kind of Cu-based MOF, has been used in many fields because of its high thermal stability, low cost, easy preparation method, and regular 3D structure [16]. Through sulfuration [15], the Cu ions within the MOF could be easily transformed into CuS in situ. So, the HKUST is suitable to be the platform for CuS.

However, the CuS@HKUST nanoparticles are poor in dispersibility, and easy to sink when deposited in water [15], which goes against the nanoparticles' antibacterial property. And polydopamine (PDA), as a kind of natural melanin, has always been used to improve the dispersibility and biosecurity of basic materials [17, 18]. Moreover, the PDA could also absorb light and produce heat, which evidently benefits the photothermal property of the nanoparticles. Furthermore, the PDA has also been widely used to improve the photocatalytic property of materials by fast transferring the photo-induced electrons. Considering all these in mind, we attempt to design a kind of effective antibacterial agent through covering the sulfuretted HKUST nanoparticles with PDA.

Herein, we synthesized an antibacterial agent, CuS@HKUST, through the simple method of in situ sulfuration, where the CuS nanoparticles were imbedded within the 3D structure of HKUST. Moreover, PDA was used to modify the surface of the nanoparticles. In this system, the CuS nanoparticles could produce heat and free radicals under light irradiation. And the PDA could improve both the photothermal and photocatalytic properties of the nanoparticles synthesized, with the reasons listed in the following. Firstly, the PDA could improve the dispersibility and light absorbance of the nanoparticles, which benefited the photothermal and photocatalytic properties of the nanoparticles. Furthermore, the PDA could produce heat under light irradiation, which also helped the production of heat. Meanwhile, the more heat produced could accelerate the carrier mobility and thus improved the photocatalytic property of the nanoparticles. Moreover, the PDA could also enhance the photocatalytic property of the nanoparticles by transferring the photo-induced electrons, which resulted in the separation of the holes and electrons. Therefore, when exposed to light irradiation, the material showed great broad-spectrum antibacterial property because of the synergistic effect of the heat and free radicals produced.

2 Experimental

2.1 Materials preparation

As a simple and easily controlled method, the solvothermal method was used to synthesize the Cu-based MOF material (HKUST), HKUST after in situ sulfuration (CuS@HKUST) and CuS@HKUST covered with polydopamine (CuS@HKUST-PDA).

HKUST nanoparticles were synthesized according to the previous report [15]. 7.74 mmol $Cu(NO_3)_2{\cdot}3H_2O$ and 4.28 mmol 1,3,5-benzenetricarboxylate (BTC) were, respectively, weighted and then dissolved in the mixture of deionized water, ethanol and dimethylformamide (DMF) at the volume ratio of 1: 1: 1 (15 ml deionized water, 15 ml ethanol, and 15 ml DMF). In order to guarantee that the agents added were fully dissolved, the mixture was sonicated for 20 min. After that, the clear solution was kept in an oven with the temperature set to 70 °C. And 7 h later, the resultant solution was cooled to room temperature, with the blue powder, HKUST nanoparticles, collected after centrifugation, washing and drying.

In order to synthesize CuS@HKUST, 0.40 g HKUST powder was immersed in 40 ml ethanol. After that, 0.60 g thioacetamide was added into the above solution. Then, the mixture was being kept in water bath for 4 h (the temperature was set to 30 °C), with stirring. Then, the sediment was collected after centrifugation, washing and drying.

For the synthesis of CuS@HKUST-PDA nanoparticles, tris–HCl (pH = 8.4) buffer was previously prepared. Then, 30 mg synthesized CuS@HKUST nanoparticles were deposited in 5 ml ethanol, followed by adding 5 ml above tris-HCl solution. Then, 10 mg dopamine was added. After 5-min stirring, the mixture was shocked in dark. And 2 h later, the CuS@HKUST-PDA was collected by centrifugation.

The morphologies of the CuS@HKUST and CuS@HKUST-PDA nanoparticles were characterized by scanning

electron microscopy (SEM, HITACHI S-4800, Tokyo, Japan). X-ray diffractometer (XRD, Bruker D8 Advance, Germany) and Fourier transform infrared spectroscopy (FTIR, AVANCE IIITMHD 400 MHz NanoBAY, China) were used to test the structure and composition of the CuS@HKUST and CuS@HKUST-PDA nanoparticles. Ultraviolet–visible (UV–Vis, UV-2700, Japan) spectrophotometer was used to represent the nanoparticles' abilities to absorb light.

2.2 Photothermal and photocatalytic measurement

In order to test the different nanoparticles' photothermal conversion ability, the photothermal curves were measured. The CuS@HKUST and CuS@HKUST-PDA nanoparticles were dispersed in PBS solution at the concentration of 300 mg·L^{-1}. Then, 200 μl above solutions were separately deposited in 96-well plate and put under 808-nm light irradiation, with the PBS solution set as the blank control. Every minute, the temperature of the solution was recorded. In order to test the photothermal stability of the nanoparticles, the solutions of different nanoparticles were exposed to light for 5 min and then moved into dark. During the repeated 3 cycles, the temperature was recorded every minute.

2',7'-dichlorofluorescein (DCF) was used as the ROS detector to test the photocatalytic property of the different nanoparticles. Firstly, the 2',7'-dichlorofluorescein diacetate (DCFH-DA) was added into 0.01 mol·L^{-1} NaOH solution. After 30-min stirring in the dark, DCF solution was obtained [19]. The CuS@HKUST and CuS@HKUST-PDA nanoparticles were dispersed in deionized water at the concentration of 300 mg·L^{-1}. Then, the prepared DCF solution was added into the solution of CuS@HKUST and CuS@HKUST-PDA, respectively. Finally, the solution was irradiated by 808 nm light, and the fluorescence intensity was measured by a microplate reader.

2.3 Antibacterial property of synthesized materials

The antibacterial properties of the CuS@HKUST and CuS@HKUST-PDA nanoparticles were represented through the method of plate spreading. Firstly, the CuS@HKUST and CuS@HKUST-PDA nanoparticles were added into the PBS (pH = 7.4) solution and dispersed by ultrasonic concussion. Then, the solutions of CuS@HKUST (300 mg·L^{-1}), CuS@HKUST-PDA (300 mg·L^{-1}) and PBS were mixed with the bacterial suspension (1×10^7 CFU·ml^{-1}). After that, the mixtures were exposed to 808-nm light irradiation or kept in the dark. And 20 min later, the suspensions were shocked and diluted. Then, 20 μl diluted solution was spread on the plate. After 24-h cultivation, the number of colonies on the plates was calculated. The antibacterial property was calculated as follows:

$$\text{Antibacterial ratio} = \left(1 - \text{CFU}_{\text{exg}}/\text{CFU}_{\text{cog}}\right) * 100\% \quad (1)$$

where CFU_{exg} is the colony-forming units (CFU) of the experimental groups, CFU_{cog} is the CFU of the control group.

3 Results and discussion

3.1 Morphology and composition of synthesized nanoparticles

Based on the previous research of our groups, the obtained CuS@HKUST nanoparticles after 4-h sulfuration showed the best antibacterial property against *Staphylococcus aureus* (*S. aureus*) and *Escherichia coli* (*E. coli*) [15]. So in this report, the CuS@HKUST used was the ones after 4-h sulfuration. After in situ sulfuration, part of the Cu ions within the HKUST nanoparticles were transferred into CuS nanoparticles. And after a simple process of auto-polymerization, the CuS@HKUST-PDA nanoparticles were synthesized, as shown in Fig. 1.

As shown in Figure S1, the CuS@HKUST nanoparticles synthesized were blue-green. While after the CuS@HKUST nanoparticles were dispersed in the solution of dopamine, the solution turned into black. And along with the reaction time increasing, the solution turned to be more and more black, indicating the auto-polymerization of polydopamine over CuS@HKUST nanoparticles. Then, SEM was used to characterize the morphologies of the different nanoparticles to confirm that the CuS@HKUST-PDA nanoparticles were successfully covered with PDA. As shown in Fig. 2, the CuS@HKUST nanoparticles synthesized were 6–12 μm in diameter. It could also be found that the CuS@HKUST nanoparticles were typically octahedral, with clear edges and corners, which was similar to the previous report [15]. The results of EDS represented that besides C, O and Cu, S could also be found in the nanoparticles, which indicated the successful synthesis of the CuS within the nanoparticles after sulfuration (Figure S2). Furthermore, the result of elemental mapping showed that similar to C, O and Cu, S also dispersed all over the nanoparticles uniformly. This meant that the CuS nanoparticles were distributed evenly throughout the nanoparticles (Figure S3). While after the CuS@HKUST nanoparticles were covered with PDA, the shape of the nanoparticles was still typically octahedral, though the size of the nanoparticles grew a little bigger (8–15 μm in diameter). However, the edge of the nanoparticles was misty. And the surface of the nanoparticles was much

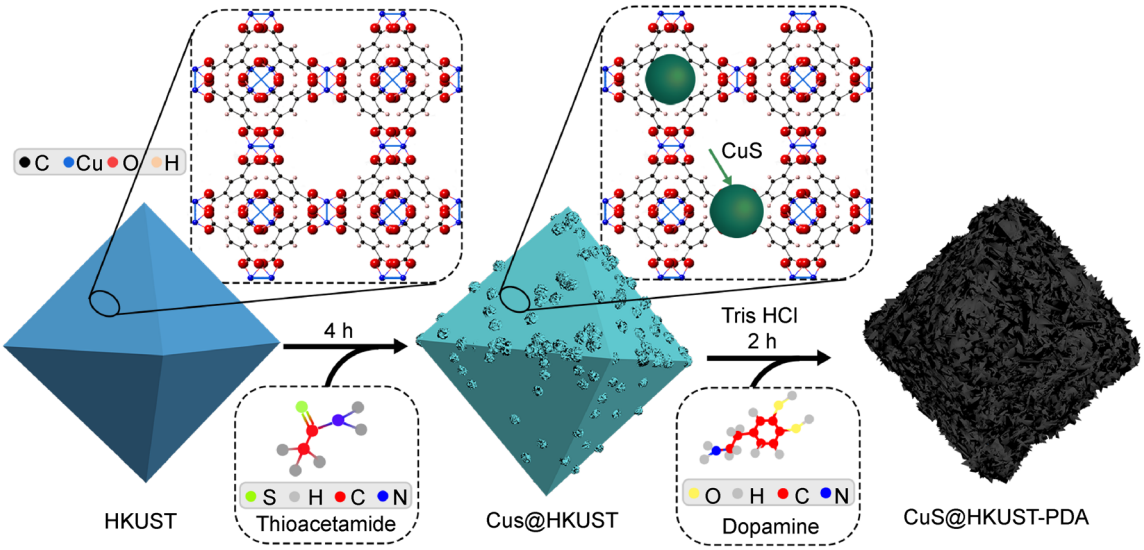

Fig. 1 Scheme illustrating synthesis process of CuS@HKUST-PDA

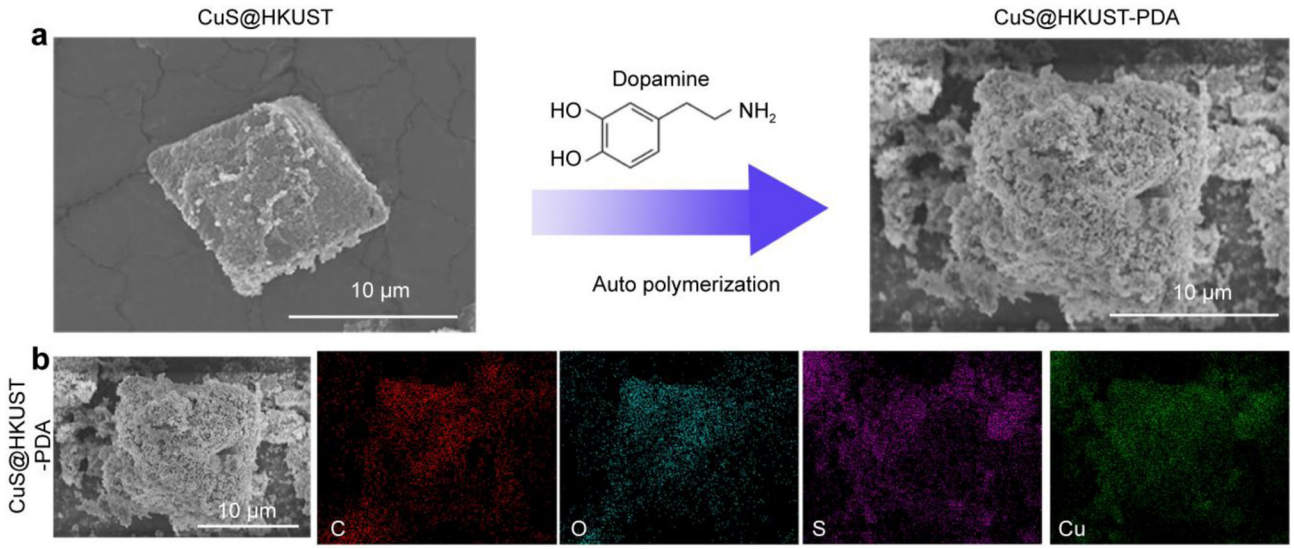

Fig. 2 **a** Morphology of CuS@HKUST and CuS@HKUST-PDA; **b** elemental mapping images of CuS@HKUST-PDA

rougher, with lots of attachment on it, as shown in Fig. 2. This obvious change indicated that the CuS@HKUST nanoparticles were fully covered with PDA. Furthermore, from the results of elemental mapping and EDS, it was obvious that all the elements C, O, Cu and S were dispersed over the nanoparticles, indicating that the PDA was equally covered above the nanoparticles.

In order to further confirm the CuS@HKUST nanoparticles were covered with PDA, FTIR was performed. As shown, in the spectrum of CuS@HKUST, obvious peaks should be found at 1645.5, 1376.5 and 1189.4 cm^{-1} (Fig. 3a), which came from the stretching vibrational of C = O, C–O and bending vibrational of O–H [20–22], representing the existence of the carboxyl group. There also existed one peak at around 730 cm^{-1}, which indicated the existence of Cu–O band. These results confirmed that the HKUST nanoparticles were synthesized. Furthermore, a peak at around 490 cm^{-1} could also be found, which originated from the stretching vibrational of Cu–S bond, confirming the successful synthesis of CuS [23]. Then, the FTIR spectrum was also performed to test the composition of CuS@HKUST-PDA. Firstly, in the spectrum, the peaks appeared to be few and narrow, but not in large number of wild, which represented that the dopamine was polymerized into polydopamine, but not existed as the monomer [24]. And it was also obvious that the peaks of CuS@HKUST-PDA were similar to those of CuS@HKUST. These came from several respects. Firstly, the functional groups

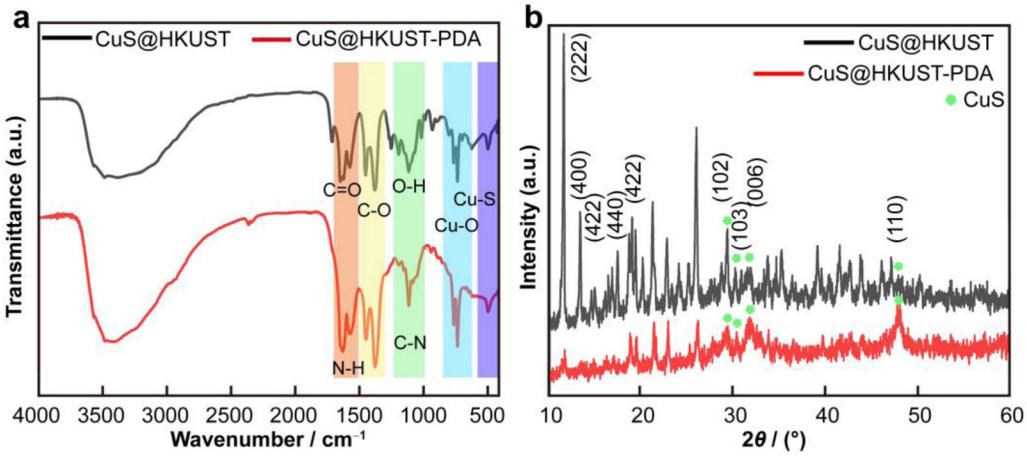

Fig. 3 **a** FTIR spectra and **b** XRD patterns of CuS@HKUST and CuS@HKUST-PDA

of PDA and 1,3,5-benzenetricarboxylic acid are alike, as shown in Figure S4. They both own benzene ring and hydroxyl groups, so the characteristic peaks might be similar. Moreover, for the CuS@HKUST-PDA, the newly appeared bonds were N–H and C–N bonds, whose peaks usually appeared around 1650–1550 and 1100–1200 cm^{-1}, which was coincident with that of COOH and O–H, respectively [25]. So, in the spectrum of CuS@HKUST-PDA, only some peaks were enhanced, but no new peaks were found. And in the spectrum of CuS@HKUST-PDA, there also existed obvious peaks at about 730 and 500 cm^{-1}, which confirmed the retention of Cu–O and Cu–S bond, respectively.

XRD was performed to test the structure of the MOFs before and after coated with polydopamine (Fig. 3b). The results showed that after modification with PDA, the structure of the nanoparticles changed. In the spectrum of CuS@HKUST, several sharp peaks could be found, confirming the structure of the HKUST and CuS. As shown in Fig. 3b, in the XRD patterns of CuS@HKUST, strong peaks were found around 11.5°, 13.4° and 18.8°. These peaks were the characteristic peaks of HKUST [20, 26], demonstrating the retention of the structure of HKUST after sulfuration. And characteristic peaks of CuS could also be found around 30° and 48°, which correspond to (102), (103), (006) and (110) crystal facets of CuS, indicating the successful synthesis of CuS [27, 28]. However, it could not be ignored, compared with the previously reported XRD pattern of the pure HKUST nanoparticles, the spectrum of the CuS@HKUST nanoparticles was a little wilder, with more small peaks appeared [26]. This was because after the process of in situ sulfuration, the synthesized CuS nanoparticles would compress and destroy the 3D structure of the HKUST, resulting in the damage of the construction, and thus the disorder of the peaks in the XRD pattern. And it was apparent that after the nanoparticles were coated with PDA, the main peaks still appeared at the same position, which confirmed the part retention of the HKUST structure, as well as the existence of CuS within nanoparticles. However, it also could not be ignored that the peaks were significantly weakened, indicating the further disorder of the structure. This was because the HKUST nanoparticles synthesized were not so stable in water [20, 29]. And during the process of modification with PDA, the HKUST nanoparticles further collapsed, resulting in the further disorder of the structure.

The nanoparticles' dispersibility in water could also confirm whether the CuS@HKUST nanoparticles were modified with PDA. The PDA was strong hydrophilic [24, 30], so if the nanoparticles were successfully covered with PDA, the dispersibility of nanoparticles might be enhanced. As shown in Fig. 4, after ultrasonic dispersion, the CuS@HKUST and CuS@HKUST-PDA nanoparticles both formed uniform turbid solution, though their colors were different. The solution containing CuS@HKUST was blue-green, while the one containing CuS@HKUST-PDA was black. This was because the PDA synthesized through the auto-polymerization of dopamine was black. So, when the CuS@HKUST nanoparticles were covered with PDA, it was rational to find that the nanoparticles turned into black. It was obvious that the dispersion of the CuS@HKUST in water was quite poor. After 5-min standing, the blue-green nanoparticles gradually sank, and the supernatant liquid appeared to be lighter. Along with the time increasing, the supernatant liquid was lighter and lighter. And 20 min later, distinct two layers could be found in the liquid, with nearly clear supernatant left. However, for CuS@HKUST-PDA, the situation was different. Even after 20-min standing, the solution still appeared to be uniform, without evident stratification. This result confirmed that the CuS@HKUST-PDA nanoparticles were successfully covered with PDA from the side.

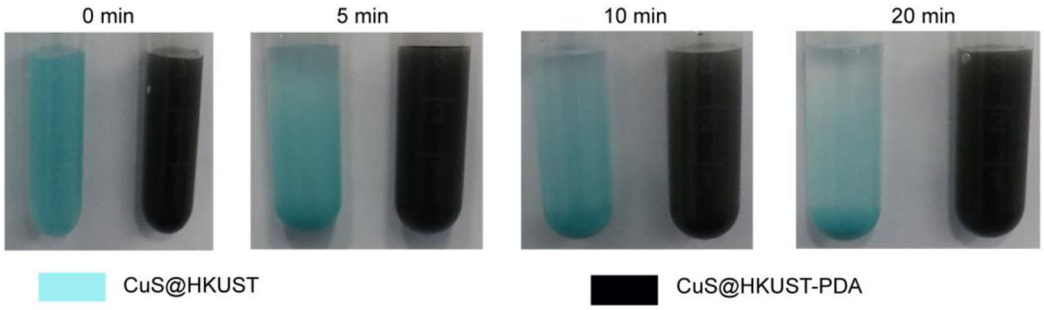

Fig. 4 Dispersibility of CuS@HKUST and CuS@HKUST-PDA in water

3.2 Photothermal and photodynamic properties of nanoparticles synthesized

After in situ sulfuration, part of the Cu clusters in the HKUST turned into CuS. Because of the photothermal and photocatalytic properties of the CuS [31, 32], it was rational to speculate that the CuS@HKUST could produce heat and free radical under 808-nm light irradiation. The ability to absorb light has great effect on the photothermal and photocatalytic properties of the nanoparticles. So, the UV–Vis spectrum was first performed. As shown in Fig. 5, it was obvious that the CuS@HKUST-PDA nanoparticles' light absorbance was much higher than that of CuS@HKUST. This was because, as a kind of photothermal agent, the PDA itself could also absorb light [33, 34]. When the PDA and CuS@HKUST were combined, it was rational to find that the nanoparticles could absorb much more light.

In order to verify the photothermal properties of the CuS@HKUST and CuS@HKUST-PDA, heating and cooling curves were performed. As shown in Fig. 6, under 808-nm light irradiation, both the CuS@HKUST and CuS@HKUST-PDA could produce heat. And it was obvious that after 5-min exposure, the temperature of CuS@HKUST solution could reach around 42 °C, while

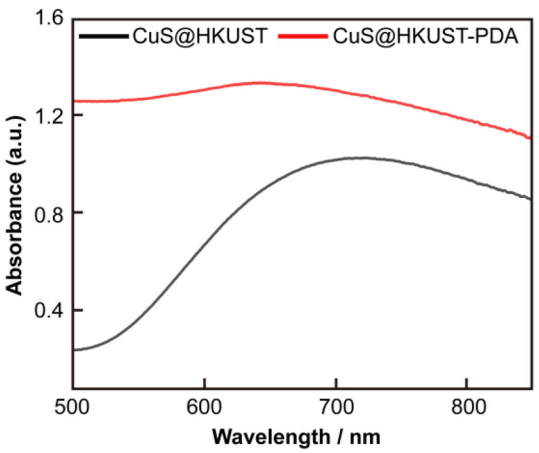

Fig. 5 UV–Vis spectra of CuS@HKUST and CuS@HKUST-PDA

that of CuS@HKUST-PDA solution could reach as high as 56–57 °C. This result represented that the photothermal conversion ability of CuS@HKUST-PDA was much higher than that of the CuS@HKUST. This came from several respects. Firstly, the CuS@HKUST-PDA could absorb much more light than the CuS@HKUST, which was beneficial for the production of heat [35, 36]. Secondly, after modification with PDA, the nanoparticles' dispersibility in water was significantly improved, which could help produce heat. More important, both the PDA and CuS@HKUST could produce heat under light irradiation [33]. So, when they were combined, it was rational to find that the photothermal conversion ability was excellently enhanced. It could also be found that when the light was moved away after 5-min irradiation, the temperature declined. And when the nanoparticles were irradiated again, the temperature increased again in a similar way. This process could be repeated several times without obvious changes, indicating that both the CuS@HKUST and CuS@HKUST-PDA had great photothermal stability.

Because of the existence of the CuS, the CuS@HKUST could also produce free radical under light irradiation [15, 37, 38]. In order to testify the influence of PDA on the photocatalytic property of CuS@HKUST nanoparticles, the DCF was used as detector to test quantitatively. The DCF could react with the free radicals and resulted in the increased intensity. So, there existed a positive correlation between the amount of free radical produced and the fluorescence intensity. As the results shown in Fig. 6b, it was obvious that after modification with PDA, the nanoparticles could produce much more free radical under light irradiation. There were several possible reasons. First, after modification with PDA, the nanoparticles' could absorb much more light at around 808 nm, which benefited the nanoparticles' photocatalytic ability [39]. Moreover, because of the unique structure, PDA could transfer the electron produced in CuS, which resulted in the prevention of the electron–hole recombination in CuS, and finally improved the photocatalytic property of the nanoparticles [40–42]. Furthermore, it could not be ignored that after modification with PDA, much more heat could be produced

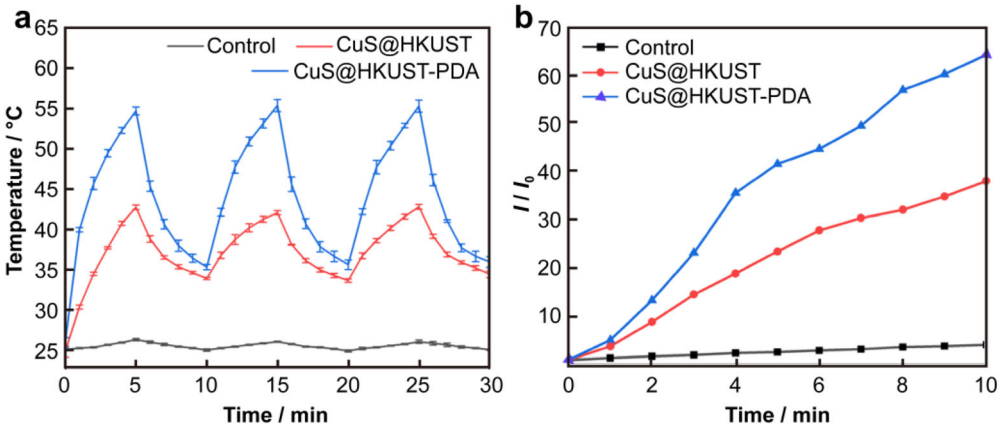

Fig. 6 Photothermal and photocatalytic properties of different nanoparticles: **a** heating and cooling curves of CuS@HKUST and CuS@HKUST-PDA under 808-nm light irradiation; **b** intensity of mixture of DCF and CuS@HKUST or the CuS@HKUST-PDA after exposure to 808-nm light irradiation (I: intensity of solution at different time points; I_0: intensity of solution at the beginning)

under light irradiation. And at higher temperature, both the carrier mobility and indirect transition were improved, which could also lead to the enhanced photocatalytic property of nanoparticles [24, 43, 44]. At last, the PDA also improved the dispersity of CuS@HKUST nanoparticles in water, which also helped the production of free radical.

3.3 Antibacterial properties of synthesized nanoparticles

S. aureus and *E. coli* were used as the model bacteria to test the antibacterial property of the CuS@HKUST and CuS@HKUST-PDA.

As shown in Fig. 7, when *S. aureus* were mixed with CuS@HKUST or CuS@HKUST-PDA and kept in the dark for 20 min, the antibacterial efficiency for CuS@HKUST and CuS@HKUST-PDA was 18.25% and 9.54%, respectively, representing that almost no bacteria were killed. This result showed that neither CuS@HKUST nor CuS@HKUST-PDA could kill *S. aureus* efficiently through short period of direct contact in darkness. However, when the *S. aureus* were mixed with the CuS@HKUST or CuS@HKUST-PDA nanoparticles and exposed to 808-nm near-infrared (NIR) light, the bacteria were killed much more efficiently. And the antibacterial property of the CuS@HKUST-PDA was much higher than that of CuS@HKUST (i.e., the antibacterial efficiency against *S. aureus* of CuS@HKUAT-PDA reached up to 99.77%, while that against *S. aureus* of CuS@HKUAT was only 51.38%). When the different nanoparticles were mixed with *E. coli*, the situation was similar (Figure S5). When kept in darkness, neither the CuS@HKUST-PDA nor the CuS@HKUST killed the bacteria efficiently (the antibacterial ratio of CuS@HKUST-PDA was 12.65%, and that of CuS@HKUST was 27.8%). When the nanoparticles were mixed with the bacteria and exposed to light, the

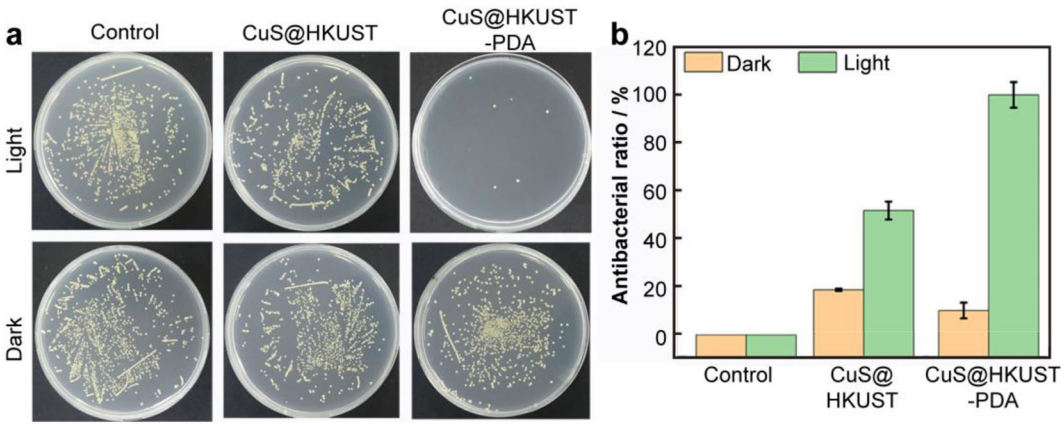

Fig. 7 Antibacterial property of CuS@HKUST and CuS@HKUST-PDA against *S. aureus*: **a** plate spreading result representing antibacterial property of different nanoparticles; **b** statistic analysis of plate spreading results

antibacterial efficiency of CuS@HKUST-PDA reached up to 99.57%, while that of CuS@HKUST was only 52.64%. This might come from several reasons listed in the following. First, under light irradiation, the CuS@HKUST-PDA could produce much more heat and free radical radicals than CuS@HKUST (Fig. 6). And as shown in Figure S6, after 20-min irradiation under light, the temperature of the CuS@HKUST-PDA could reach nearly up to 65 °C finally, while the CuS@HKUST could only reach around 48 °C. So, when the bacteria were mixed with CuS@HKUST-PDA, the cell membrane, DNA, and functional proteins would be attacked and significantly damaged by the combination of high temperature and a large number of free radicals [32], as shown in Fig. 8. Furthermore, for the CuS@HKUST-PDA, because of the existence of PDA, the nanoparticles' interaction with the bacteria was enhanced, which also benefited the attack of free radicals and heat against bacteria. So, based on all these above, the CuS@HKUST-PDA showed excellent broad-spectrum antibacterial property.

4 Conclusion

In this paper, the highly efficient antibacterial material of CuS@HKUST-PDA was designed. The Cu-based MOF, HKUST was chosen as the basic material because its Cu clusters could be transferred to CuS nanoparticles through the simple process of in situ sulfuration. In this way, the CuS nanoparticles were immobilized within the MOF structure and could not gather with each other. And in order to further improve the photothermal property of the nanoparticles, PDA was used to modify the surface of the nanoparticles, which could produce lots of heat under light irradiation. Moreover, the PDA could also benefit heat production by improving the dispersibility and light absorbance of the nanoparticles. More importantly, the PDA could also transfer the photo-induced electrons produced and thus prevent the recombination of holes and electrons, resulting in the enhanced photocatalytic property of the nanoparticles. Under the combination of the more heat and free radicals, the CuS@HKUST-PDA

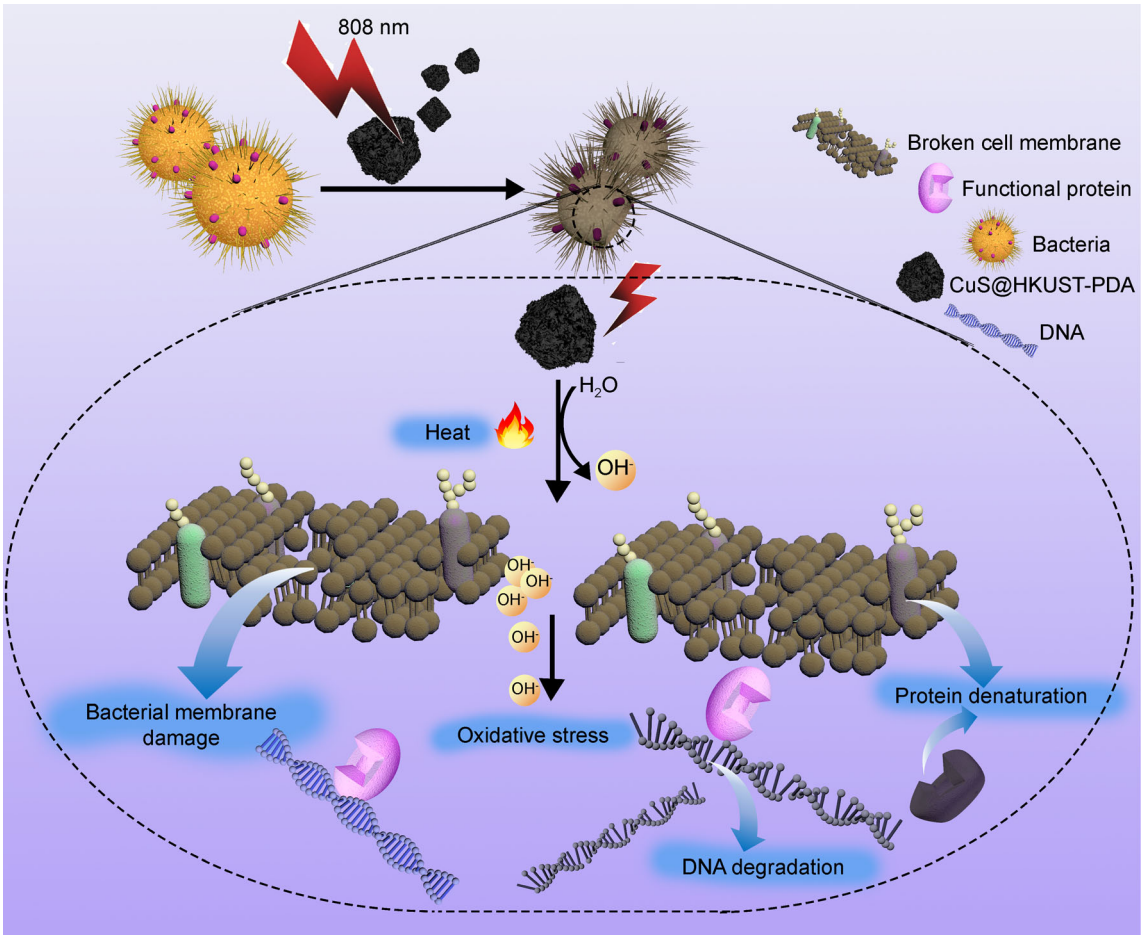

Fig. 8 Scheme illustrating mechanism of CuS@HKUST-PDA killing bacteria

nanoparticles showed excellent broad-spectrum antibacterial and had great potential to act as kind of antibiotic-free antibacterial agent in many fields, such as instrument disinfection and environment depollution.

Acknowledgements This work was financially supported by Jilin Provincial Science and Technology Project (No. YDZJ202101-ZYTS054), the National Science Fund for Distinguished Young Scholars (No. 51925104) and the National Natural Science Foundation of China (No. 51871162).

References

[1] Liu X, Li X, Shan Y, Yin Y, Liu C, Lin Z, Kumar SS. CuS nanoparticles anchored to g-C_3N_4 nanosheets for photothermal ablation of bacteria. RSC Adv. 2020;10(21):12183.
[2] Farrow C, McBean E, Huang G, Yang AL, Wu YC, Liu Z, Dai ZN, Cawte T, Li YP. Ceramic water filters: a point-of-use water treatment technology to remove bacteria from drinking water in Longhai city, Fujian province, China. J Environ Inform. 2018; 32(2):63.
[3] Brown ED, Wright GD. Antibacterial drug discovery in the resistance era. Nature. 2016;529(7586):336.
[4] Theuretzbacher U, Outterson K, Engel A, Karlen A. The global preclinical antibacterial pipeline. Nat Rev Microbiol. 2020; 18(5):275.
[5] Levy SB, Marshall B. Antibacterial resistance worldwide: causes, challenges and responses. Nat Med. 2004;10(12 Suppl): S122.
[6] Dai B, Yu Y, Chen Y, Huang H, Lu C, Kou J, Zhao Y, Xu Z. Construction of self-healing internal electric field for sustainably enhanced photocatalysis. Adv Funct Mater. 2019;29(16): 1807934.
[7] Gao L, Cui X, Wang Z, Sewell C, Li Z, Liang S, Zhang M, Li J, Hu Y, Lin Z. Operando unraveling photothermal-promoted dynamic active-sites generation in $NiFe_2O_4$ for markedly enhanced oxygen evolution. PNAS. 2021;118(7):e2023421118.
[8] Lin Y, Han D, Li Y, Tan L, Liu X, Cui Z, Yang X, Li Z, Liang Y, Zhu S, Wu S. Ag_2S@WS_2 heterostructure for rapid bacteria-killing using near-infrared light. ACS Sustainable Chem Eng. 2019;7(17):14982.
[9] Ren Y, Liu H, Liu X, Zheng Y, Li Z, Li C, Yeung K, Zhu S, Liang Y, Cui Z, Wu S. Photoresponsive materials for antibacterial applications. Cell Rep Phys Sci. 2020;1(11):100245.
[10] Han D, Li Y, Liu X, Li B, Han Y, Zheng Y, Yeung KWK, Li C, Cui Z, Liang Y, Li Z, Zhu S, Wang X, Wu S. Rapid bacteria trapping and killing of metal-organic frameworks strengthened photo-responsive hydrogel for rapid tissue repair of bacterial infected wounds. Chem Eng J. 2020;396:125194.
[11] Ding H, Han D, Han Y, Liang Y, Liu X, Li Z, Zhu S, Wu S. Visible light responsive CuS/ protonated g-C_3N_4 heterostructure for rapid sterilization. J Hazard Mater. 2020;393:122423.
[12] Li Y, Liu X, Tan L, Cui Z, Yang X, Zheng Y, Yeung KWK, Chu PK, Wu S. Rapid sterilization and accelerated wound healing using Zn^{2+} and graphene oxide modified g-C_3N_4 under dual light irradiation. Adv Funct Mater. 2018;28(30):1800299.
[13] Zhao Y, Liu J, Han M, Yang G, Ma L, Wang Y. Two comparable Ba-MOFs with similar linkers for enhanced CO_2 capture and separation by introducing N-rich groups. Mater Rare Met. 2021;40(2):499.
[14] Li Y, Yang Y, Huang J, Wang L, She H, Zhong J, Wang Q. Preparation of CuS/$BiVO_4$ thin film and its efficaciously photoelectrochemical performance in hydrogen generation. Rare Met. 2019;38(5):428.
[15] Yu P, Han Y, Han D, Liu X, Liang Y, Li Z, Zhu S, Wu S. In-situ sulfuration of Cu-based metal-organic framework for rapid near-infrared light sterilization. J Hazard Mater. 2020;390: 122126.
[16] Tan H, Li Q, Zhou Z, Ma C, Song Y, Xu F, Wang L. A sensitive fluorescent assay for thiamine based on metal-organic frameworks with intrinsic peroxidase-like activity. Anal Chim Acta. 2015;856:90.
[17] Yu S, Li G, Liu R, Ma D, Xue W. Dendritic Fe_3O_4@poly(-dopamine)@PAMAM nanocomposite as controllable NO-releasing material: a synergistic photothermal and NO antibacterial study. Adv Funct Mater. 2018;28(20):1707440.
[18] Kim Y, Coy E, Kim H, Mrowczynski R, Torruella P, Jeong D, Choi KS, Jang JH, Song MY, Jang D, Peiro F, Jurga S, Kim HJ. Efficient photocatalytic production of hydrogen by exploiting the polydopamine-semiconductor interface. Appl Catal B. 2021; 280:119423.
[19] Han D, Ma M, Han Y, Cui Z, Liang Y, Liu X, Li Z, Zhu S, Wu S. Eco-friendly hybrids of carbon quantum dots modified MoS_2 for rapid microbial inactivation by strengthened photocatalysis. ACS Sustainable Chem Eng. 2019;8(1):534.
[20] Tian N, Gao Y, Wu J, Luo S, Dai W. Water-resistant HKUST-1 functionalized with polydimethylsiloxane for efficient rubidium ion capture. New J Chem. 2019;43(39):15539.
[21] Wang C, Qian X, An X. In situ green preparation and antibacterial activity of copper-based metal-organic frameworks/cellulose fibers (HKUST-1/CF) composite. Cellulose. 2015;22(6):3789.
[22] Mosleh S, Rahimi MR, Ghaedi M, Dashtian K, Hajati S. Photocatalytic degradation of binary mixture of toxic dyes by HKUST-1 MOF and HKUST-1-SBA-15 in a rotating packed bed reactor under blue LED illumination: central composite design optimization. RSC Adv. 2016;6(21):17204.
[23] Gupta VK, Pathania D, Agarwal S, Singh P. Adsorptional photocatalytic degradation of methylene blue onto pectin-CuS nanocomposite under solar light. J Hazard Mater. 2012;243:179.
[24] Han D, Li Y, Liu X, Yeung KWK, Zheng Y, Cui Z, Liang Y, Li Z, Zhu S, Wang X, Wu S. Photothermy-strengthened photocatalytic activity of polydopamine-modified metal-organic frameworks for rapid therapy of bacteria-infected wounds. J Mater Sci Technol. 2021;62:83.
[25] Feng M, Yu S, Wu P, Wang Z, Liu S, Fu J. Rapid, high-efficient and selective removal of cationic dyes from wastewater using hollow polydopamine microcapsules: isotherm, kinetics, thermodynamics and mechanism. Appl Surf Sci. 2021;542:148633.
[26] Cui X, Sun X, Liu L, Huang Q, Yang H, Chen C, Nie S, Zhao Z, Zhao Z. In-situ fabrication of cellulose foam HKUST-1 and surface modification with polysaccharides for enhanced selective adsorption of toluene and acidic dipeptides. Chem Eng J. 2019;369:898.
[27] Song C, Wang X, Zhang J, Chen X, Li C. Enhanced performance of direct Z-scheme CuS-WO_3 system towards photocatalytic decomposition of organic pollutants under visible light. Appl Surf Sci. 2017;425:788.
[28] Qin Y, Kong X, Lei D, Lei X. Facial grinding method for synthesis of high-purity CuS nanosheets. Ind Eng Chem Res. 2018;57(8):2759.
[29] Álvarez JR, Sánchez-González E, Pérez E, Schneider-Revueltas E, Martínez A, Tejeda-Cruz A, Islas-Jácome A, González-Zamora E, Ibarra IA. Structure stability of HKUST-1 towards water and ethanol and their effect on its CO_2 capture properties. Dalton Trans. 2017;46(28):9192.
[30] Liu Y, Ai K, Lu L. Polydopamine and its derivative materials: Synthesis and promising applications in energy, environmental, and biomedical fields. Chem Rev. 2014;114(9):5057.

[31] Li L, Rashidi LH, Yao M, Ma L, Chen L, Zhang J, Zhang Y, Chen W. CuS nanoagents for photodynamic and photothermal therapies: phenomena and possible mechanisms. Photodiagn Photodyn Ther. 2017;19:5.
[32] Li M, Liu X, Tan L, Cui Z, Yang X, Li Z, Zheng Y, Yeung K, Chu PK, Wu S. Noninvasive rapid bacteria-killing and acceleration of wound healing through photothermal/photodynamic/copper ion synergistic action of a hybrid hydrogel. Biomater Sci. 2018;6(8):2110.
[33] Ding X, Liu J, Li J, Wang F, Wang Y, Song S, Zhang H. Polydopamine coated manganese oxide nanoparticles with ultrahigh relaxivity as nanotheranostic agents for magnetic resonance imaging guided synergetic chemo-/photothermal therapy. Chem Sci. 2016;7(11):6695.
[34] Chen Y, Ai K, Liu J, Ren X, Jiang C, Lu L. Polydopamine-based coordination nanocomplex for T1/T2 dual mode magnetic resonance imaging-guided chemo-photothermal synergistic therapy. Biomaterials. 2016;77:198.
[35] Zou Y, Wu T, Li N, Guo X, Li Y. Photothermal-enhanced synthetic melanin inks for near-infrared imaging. Polymer. 2020;186:122042.
[36] Tian Y, Zhang J, Tang S, Zhou L, Yang W. Polypyrrole composite nanoparticles with morphology-dependent photothermal effect and immunological responses. Small. 2016;12(6):721.
[37] Hou L, Shan X, Hao L, Feng Q, Zhang Z. Copper sulfide nanoparticle-based localized drug delivery system as an effective cancer synergistic treatment and theranostic platform. Acta Biomater. 2017;54:307.
[38] Xu W, Zhu S, Liang Y, Li Z, Cui Z, Yang X, Inoue A. Nanoporous CuS with excellent photocatalytic property. Sci Rep. 2015;5(1):1.
[39] Hou L, Zhang M, Guan Z, Li Q, Yang J. Effect of annealing ambience on the formation of surface/bulk oxygen vacancies in TiO_2 for photocatalytic hydrogen evolution. Appl Surf Sci. 2018;428:640.
[40] Sun X, Yan L, Xu R, Xu M, Zhu Y. Surface modification of TiO_2 with polydopamine and its effect on photocatalytic degradation mechanism. Colloids Surf A. 2019;570:199.
[41] Zhang C, Yang H, Wan L, Liang H, Li H, Xu Z. Polydopamine-coated porous substrates as a platform for mineralized β-FeOOH nanorods with photocatalysis under sunlight. ACS Appl Mater Interfaces. 2015;7(21):11567.
[42] Huo R, Yang X, Yang J, Yang S, Xu Y. Self-assembly synthesis of $BiVO_4$/polydopamine/g-C_3N_4 with enhanced visible light photocatalytic performance. Mater Res Bull. 2018;98:225.
[43] Wang X, He Y, Hu Y, Jin G, Jiang B, Huang Y. Photothermal-conversion-enhanced photocatalytic activity of flower-like CuS superparticles under solar light irradiation. Sol Energy. 2018;170:586.
[44] Dai B, Fang J, Yu Y, Sun M, Huang H, Lu C, Kou J, Zhao Y, Xu Z. Construction of infrared-light-responsive photoinduced carriers driver for enhanced photocatalytic hydrogen evolution. Adv Mater. 2020;32(12):1906361.